Dynamics of Excited States of the Carotenoid Peridinin in Polar Solvents: Dependence on Excitation Wavelength, Viscosity, and Temperature

Donatas Zigmantas,[†] Roger G. Hiller,[‡] Arkady Yartsev,[†] Villy Sundström,[†] and Tomáš Polívka*,[†]

Department of Chemical Physics, Lund University, Box 124, S-22100 Lund, Sweden, and Department of Biological Sciences, Macquarie University, NSW, Australia 2109

Received: October 17, 2002; In Final Form: February 18, 2003

The dynamics of the excited states of the carotenoid peridinin in polar solvents were studied using femtosecond transient absorption spectroscopy in the spectral range of 500−1900 nm. A broadening of the absorption spectrum in polar solvents is caused by a distribution of conformers having different ground-state properties. In addition, the dependence of the peridinin lifetime on the excitation wavelength reveals that two peridinin forms coexist in protic solvents, where a "red"-absorbing form is produced by hydrogen bonding via the carbonyl group. The observed dynamics show that the S_1 and intramolecular charge transfer (ICT) states of peridinin are strongly coupled, forming a collective S_1/ICT state whose lifetime is determined by the degree of ICT character. In nonpolar solvent, pure S_1 character with a lifetime of ∼160 ps is observed, whereas in polar solvents an increase in the ICT character leads to a lifetime as short as 10 ps in methanol and 13 ps in ethylene glycol. In protic solvents, the ICT character of the S_1/ICT state of the red peridinin form is further enhanced by hydrogen bonding, resulting in lifetimes shorter than 6 ps. A weak dependence of peridinin dynamics on viscosity shows that the ICT state is not formed via a twisted ICT mechanism. At 190 K in methanol, a significant increase in the S_1/ICT lifetime is observed, suggesting that thermal coupling is involved in the S_1/ICT state mixing. At 77 K in ethylene glycol glass, a multiexponential decay is revealed, indicating the presence of several conformers with different S_1/ICT state properties.

1. Introduction

Peridinin belongs to a highly substituted group of carotenoids whose spectroscopic properties are markedly affected by the presence of a carbonyl group in their structure.[1] Carbonyl carotenoids are common in various groups of marine algae where they participate in photosynthetic light-harvesting.[2] Interest in the spectroscopic properties of peridinin has greatly increased since the structure of the water-soluble light-harvesting peridinin chlorophyll protein (PCP) from *Amphidinium carterae* was resolved to 2.0 Å.[3] In the crystal, PCP consists of a trimer of identical subunits, each of which contains eight peridinins and two chlorophyll-*a* (Chl-*a*) molecules.[3] Thus, in contrast to other light-harvesting complexes, a carotenoid is the main light-harvesting pigment in the PCP complex. It was found that the overall efficiency of energy transfer from peridinin to Chl-*a* reaches almost 90%[4] and that the main part of the energy flows via the lowest excited state of peridinin.[4−6] This contrasts with the situation in light-harvesting complexes from higher plants and bacteria, where the higher excited states of carotenoids are usually the principal donors of energy in the process of carotenoid−(bacterio)chlorophyll energy transfer.[7,8]

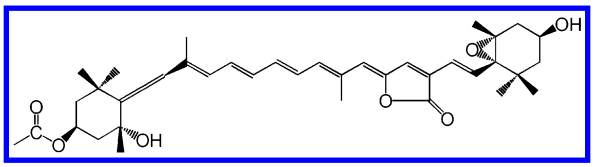

* Corresponding author. E-mail: tomas.polivka@chemphys.lu.se. Fax: +46-46-2224119.
[†] Lund University.
[‡] Macquarie University.

Spectroscopic properties of carotenoid excited states are mainly determined by the symmetry of the carotenoid conjugated chain, which, assuming a perfect symmetry, belongs to the C_{2h} point group.[9] In such a case, the S_0, S_1, and S_2 states of a carotenoid molecule have symmetry $1A_g^-$, $2A_g^-$, and $1B_u^+$, respectively, resulting in a forbidden S_0-S_1 transition. The S_0-S_2 transition is allowed and accounts for the strong absorption of carotenoids in the 400−550 nm spectral region.[9] Given the forbidden character of the S_0-S_1 transition, carotenoids usually exhibit an extremely weak S_1 fluorescence. However, for carotenoids with a carbonyl group in their conjugated chain, it was shown that they display a stronger S_1 emission than their analogues without a carbonyl group.[10] In the case of peridinin, whose conjugation length is approximately 8, the S_1 emission is unusually strong, with a fluorescence quantum yield of $\sim 10^{-3}$ in nonpolar solvents.[11] The intensity of the peridinin S_1 emission depends on solvent polarity, and the yield drops to $\sim 10^{-5}$ in polar solvents.[11] Time-resolved studies revealed that the polarity-dependent change in the S_1 emission yield is connected with a dramatic change in the lifetime of the peridinin lowest excited state, which is 160 ps in nonpolar solvents, whereas in polar solvents the lifetime may be as short as 10 ps.[11,12] This atypical behavior was explained by the presence of an intramolecular charge-transfer (ICT) state occurring in the vicinity of the peridinin S_1 state.[1,11,12] It was also established that the polarity-dependent lifetime is a common feature of carotenoids containing a carbonyl group in conjugation with the carbon−carbon conjugated chain, although the effect is most pronounced for peridinin.[1,13] The polarity-dependent lifetime was also observed for a synthetic dicyano-apo-β-carotene, suggesting that the presence of electron-withdrawing groups in the conjugated chain is the main reason for the polarity-dependent lifetime.[14]

10.1021/jp0272318 CCC: $25.00
Published on Web 05/09/2003

In addition to the S_1 lifetime dependency, a striking difference between both steady-state and transient absorption spectra in polar and nonpolar solvents is observed for peridinin and other carbonyl carotenoids[1,11] as well as for a series of apocarotenoids with a terminal carbonyl group.[13] In the steady-state absorption spectra, the characteristic three-peak vibrational structure of the carotenoid S_0-S_2 transition is lost in polar solvents and replaced by a rather structureless absorption band, usually asymmetrically broadened toward lower energies. This asymmetric broadening was also observed for the fluorescence emission.[12] Even more pronounced polarity-induced changes were revealed in the transient absorption spectra of peridinin. In the visible spectral range (480−750 nm), the transient absorption spectrum of peridinin in the nonpolar solvent *n*-hexane is dominated by a narrow excited-state absorption (ESA) band around 510 nm, attributed to the S_1-S_n transition, whereas in the polar solvent methanol it exhibits a broad ESA band centered at 590 nm, extending from 500 to 700 nm with hints of shoulders located at 525 and 630 nm.[1,11,12] Interestingly, no lifetime dependence on the probing wavelength was observed: all of the spectral features decayed with a 10-ps time constant. An extension of the transient absorption spectra toward the infrared spectral region revealed further differences between polar and nonpolar solvents. For peridinin in *n*-hexane, the spectral region of 750−1900 nm is dominated by the ESA signal above 1200 nm,[12] which is characteristic of the S_1-S_2 transition of carotenoids.[15] In methanol, a new negative spectral band located at 950 nm appears and was assigned to a stimulated emission from the peridinin ICT state,[12] showing that probing the infrared spectral region permits us to study of the ICT state without interference with signals from other excited states. The kinetics measured at the maximum of the ICT emission revealed an additional 1-ps rise component, whereas no such component was observed above 1400 nm, where the S_1-S_2 ESA dominates.[12] Dynamics occurring on the ∼1-ps time scale were also observed in the visible spectral region, where changes in the spectral profile of the peridinin ESA band in methanol occur.[12]

Several models have been proposed to explain the unusual properties of the excited states of peridinin. Bautista et al. suggested that in polar solvents the peridinin ICT state lies below the S_1, allowing efficient quenching of the S_1 state and a consequent shortening of the S_1 lifetime.[11] A small energy gap allowing thermal coupling between the S_1 and ICT states was proposed to account for the fact that the peridinin lifetime did not depend on the probing wavelength.[1,11] To explain the ∼1-ps rise of the ICT emission, a different model for peridinin excited-state dynamics was proposed.[12] In this model, the 10-ps process was ascribed to the S_1-ICT transfer driven by a polarity-controlled barrier between the S_1 and ICT states. The 1-ps dynamic was attributed to a fast relaxation of the ICT state to the ground state of peridinin. By modeling the recorded kinetics, this second model could successfully explain the observed results.[12]

The structural origin of the peridinin ICT state is still a matter of debate. Originally, the ICT state was ascribed to the presence of a lactone ring,[11] but later studies of other carbonyl carotenoids showed that the presence of the carbonyl group alone is sufficient for the observed sensitivity to solvent polarity.[1,13] However, the presence of the lactone ring or allene moiety occurring in the peridinin molecular structure can greatly enhance the solvent effect. Thus, it is the interaction of the carbonyl group with solvent molecules that leads to a stabilization of the ICT state in a polar solvent. It was also proposed that the stabilization of the ICT state might include a twisting of the molecule forming a twisted ICT (TICT),[11] as shown in DMABN dyes, for example.[16] However, spectral features similar to those observed for peridinin were also detected in the transient absorption spectra of certain push−pull polyenes, where it was shown that the twisting of the molecule is highly unlikely.[17]

In this paper, we examine the effects of the environment and excitation wavelength on the dynamics of the excited states of peridinin in polar solvents to obtain more information about its spectroscopic and dynamic properties and to test the models described above. Some properties of the models proposed above are expected to be affected by quantities studied here: (1) If a polarity-controlled barrier is involved, one would expect a strong temperature dependence of the presumptive S_1-ICT transfer rate. (2) Temperature will also alter the peridinin dynamics if thermal coupling occurs between the S_1 and ICT states. (3) The change in viscosity should have a great effect if the ICT state is formed by a TICT mechanism. (4) The excitation wavelength dependence is anticipated to give information about asymmetric broadening of the peridinin steady-state absorption spectrum. The present work shows that the dynamics of the peridinin molecule is more complex than previously thought and that in polar solvents there is a mixture of peridinin forms exhibiting different ICT state dynamics.

2. Materials and Methods

Peridinin was extracted from thylakoid membranes of *A. carterae* and purified as described in ref 12. Prior to the experiments, dried peridinin samples stored in the dark at −40 °C were dissolved in different solvents (purchased from Merck) to yield an optical density (OD) of about 0.4 at the absorption maximum. For most of the experiments, a 2-mm optical path length glass cuvette was used. In the case of peridinin in ethylene glycol, it was found that the sample slightly degrades in a standard cuvette. A 2-mm quartz rotational cuvette was substituted in this situation. The degradation of peridinin during the measurements was less than 5% in all cases as measured by the OD change at the absorption maximum. Steady-state absorption spectra were monitored regularly during the experiments, and a fresh sample was prepared when the degradation reached a value of about 5% of the initial OD.

Low-temperature measurements of peridinin in methanol were made with the 2-mm glass cuvette inserted into an optical cryostat equipped with a temperature controller enabling a precise adjustment of the sample temperature. Since methanol does not form a transparent low-temperature glass, the temperature was kept at 190 K (±0.5 K), about 10 K above the freezing point of methanol. For peridinin in ethylene glycol, the low-temperature measurements were performed at 77 K in a 3-mm path length acrylic cuvette. Using the acrylic cuvette enables the formation of a transparent ethylene glycol glass without cracking the sample.

The femtosecond spectrometer used for the experiments has been described in detail elsewhere.[12] Briefly, for measurements in the near-infrared spectral region, a commercial femtosecond system consisting of a Ti:sapphire oscillator and a Ti:sapphire regenerative amplifier operating at a repetition rate of 5 kHz producing ∼120-fs pulses centered at 800 nm was used. These pulses are used to pump two independent optical parametric amplifiers for the generation of pump and probe pulses. The parametric amplifier used for the generation of probe pulses was controlled by a computer, enabling direct scanning of the probe pulses over the spectral region of 750−1850 nm. A detection system based on a three-diode arrangement in combination with a single grating monochromator providing

TABLE 1: Solvent Polarity Factors $P(\epsilon)$, Solvent Polarizability Factors $R(n)$, and Viscosity η of the Used Solvents[a]

solvent	$P(\epsilon)$	$R(n)$	η [cp]
ethylene glycol	0.923	0.257	19.9
acetonitrile	0.921	0.21	0.345
methanol	0.913	0.202	0.597
n-hexane	0.229	0.229	0.326

[a] The solvent polarity and polarizability factors were determined from the dielectric constants ϵ and indices of refraction n according to the expressions $P(\epsilon) = (\epsilon - 1)/(\epsilon + 2)$ and $R(n) = (n^2 - 1)/(n^2 + 2)$, respectively. All of the listed parameters represent values at 20 °C.

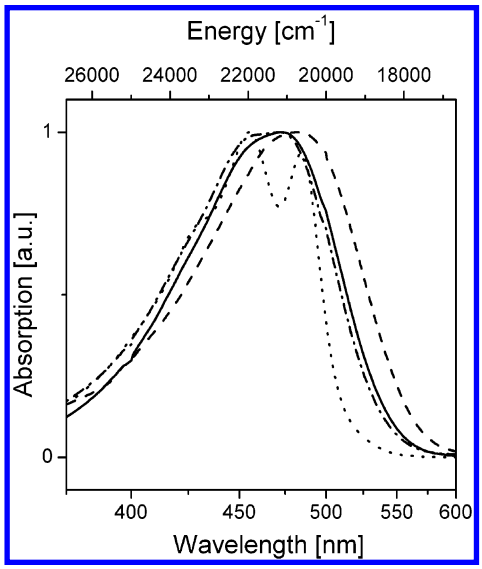

Figure 1. Absorption spectra of peridinin in *n*-hexane (•••), acetonitrile (− • −), methanol (—), and ethylene glycol (− − −). All spectra are normalized.

spectral resolution better than 40 cm^{-1} was used. For measurements in the visible range, a similar system operating at a repetition rate of 1 kHz was employed. The pump pulses were produced in the same way as for measurements in the near-infrared region, whereas a white-light continuum generated in a 0.5-cm sapphire plate was used for probing. The probe pulses were dispersed by a spectrograph onto a 512-segment photodiode array enabling direct measurements of a 270-nm-broad spectrum with a spectral resolution of ~120 cm^{-1} in each laser shot. The energy of the pump pulses was kept below 10^{14} photons $pulse^{-1}$ cm^{-2} in the case of measurements in the near-infrared spectral region. Because of a lower signal/noise ratio and lower sensitivity of the photodiode array, it was necessary to use pump pulses with higher energy, reaching in some cases 10^{15} photons $pulse^{-1}$ cm^{-2}, to obtain noise-free traces in the visible spectral region. Measurements of kinetics at different energies demonstrated that varying the intensity of pump pulses by an order of magnitude did not affect the observed dynamics. The instrument response function was 160−180 fs, depending slightly on the wavelength of probing pulses. In all measurements, the mutual polarization of the pump and probe beams was set to the magic angle (54.7°) using a polarization rotator placed in the pump beam path.

3. Results

Steady-state absorption spectra of peridinin dissolved in different solvents (for solvent parameters, see Table 1) are shown in Figure 1. In the nonpolar solvent *n*-hexane, the absorption spectrum exhibits the well-resolved structure of vibrational bands of the strongly allowed S_0-S_2 transition. Besides the striking difference between the absorption spectra of peridinin measured in polar and nonpolar solvents, it is obvious that there are subtle differences between the various polar solvents. In methanol, the absorption spectrum has a maximum around 473 nm, whereas in ethylene glycol the maximum is red-shifted to 483 nm, which represents an energy difference of ~450 cm^{-1}. In acetonitrile, the shape of the absorption spectrum resembles that measured in methanol, although it is slightly blue-shifted. In all polar solvents, the loss of vibrational structure is obvious, but it is worth noting that a hint of shoulder is preserved in methanol and acetonitrile, whereas in ethylene glycol the absorption spectrum is completely structureless with a broad red tail extending to 600 nm.

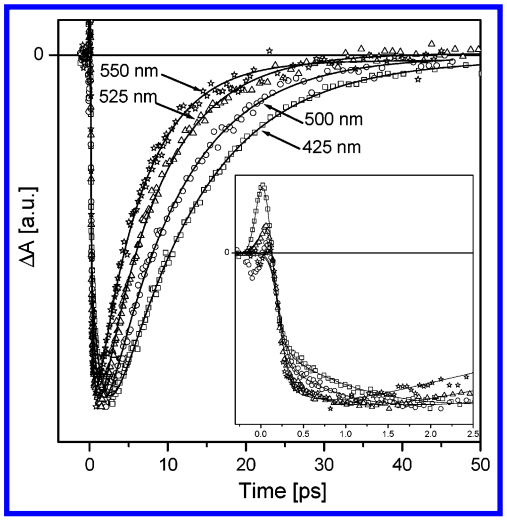

Figure 2. Kinetics recorded for peridinin in methanol at the ICT state emission maximum at 950 nm after excitation at 425 nm (□), 500 nm (○), 525 nm (△), and 550 nm (☆). All kinetics are normalized, and corresponding fits of the kinetics are represented by solid lines. An enlargement of the early-time dynamics is shown in the inset.

To explore further the kinetic consequences of the broadening of the absorption spectrum, peridinin dynamics were recorded after tuning the excitation wavelength toward the low-energy edge of the absorption band. Kinetics measured at the maximum of the ICT emission in methanol after excitation at different wavelengths are shown in Figure 2, where it is clear that the ICT emission decays faster as the excitation approaches the red tail of the absorption spectrum. Excitation at 425 nm, which represents excitation into higher vibrational levels of the S_2 state, results in a decay of the 950-nm signal with a time constant of 11 ps, whereas the decay after excitation at the red edge of the absorption spectrum at 550 nm is characterized by a 5.9-ps time constant. In addition, the rise of the ICT band becomes faster and less pronounced with excitation into the red tail of the S_0-S_2 transition, having time constants of 1.5 ps (425-nm excitation) and 0.4 ps (550 nm), respectively. It is also worth noting that excitation into the blue part of the absorption spectrum produces a positive signal at very early times because of the S_2-S_n ESA, which is known to occur in the 800−1300 nm spectral region.[12,18,19] As can be seen from the inset in Figure 2, this ESA signal is stronger when the higher vibrational levels of the S_2 state are excited.

The dependence of peridinin dynamics on excitation wavelength was also studied for several solvents in addition to methanol as shown in Figure 3, where the lifetimes are normalized to the longest observed decay for each solvent. The actual lifetimes before normalization are summarized in Table

TABLE 2: Excitation Wavelength Dependence of the Peridinin Dynamics Measured at 950 nm for Various Solvents[a]

	ethylene glycol		methanol		acetonitrile		*n*-hexane[b]	
λ_{exc} [nm]	τ_{rise} (*A*)	τ_{decay}	τ_{rise} (*A*)	τ_{decay}	τ_{rise} (*A*)	τ_{decay}	τ_{rise}	τ_{decay}
425	1 (38%)	13.7	1.5 (25%)	11				
450	0.95 (36%)	13.8	1.3 (30%)	10.5				
475	1 (36%)	12.5	1.2 (30%)	10.8	0.65 (58%)	8.2		160
500	0.65 (30%)	11.6	1 (47%)	9.6	0.66 (59%)	8.2		
525	0.6 (29%)	9.7	0.6 (23%)	7.5	0.45 (52%)	8.3		160
535	0.4 (23%)	8.4	0.6 (27%)	6.8	0.6 (41%)[c]	7.9[c]		
550	0.2 (25%)	6.1	0.4 (26%)	5.9				
570	0.15 (32%)	5.3						

[a] All time constants are listed in picoseconds. Amplitudes of the rise component are shown in parantheses. The rest of the rise occurs within the response function of the experimental setup. All of the decays are monoexponential. Uncertainties of the lifetimes and amplitudes are within ±5%. [b] Kinetics were recorded at 1700 nm because of the lack of 950-nm band in *n*-hexane. [c] Kinetics were recorded after excitation at 540 nm.

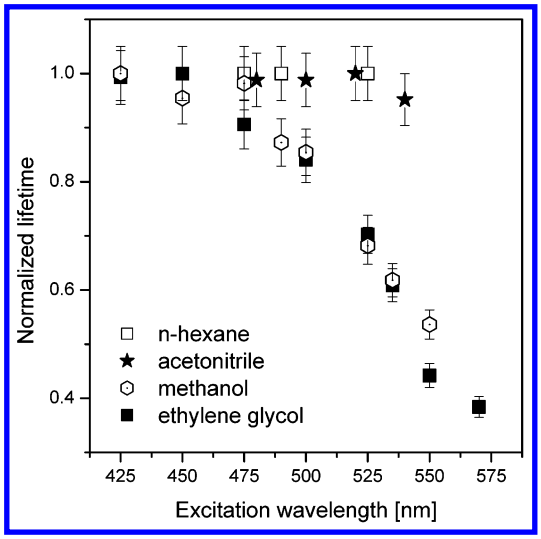

Figure 3. Dependence of peridinin lifetime on excitation wavelength in different solvents. The lifetimes are normalized to the longest observed lifetime in the corresponding solvents. See the text for details.

2. For all solvents except *n*-hexane, the lifetime dependence was probed close to the maximum of the ICT emission at 950 nm. In the case of peridinin in *n*-hexane, where no ICT band was detected, kinetics were recorded at 1700 nm (S_1-S_2 transition), where they exhibit an ~160 ± 10 ps decay independently of the excitation wavelength. The behavior of peridinin in a nonpolar solvent is similar to the behavior of carotenoids without carbonyl groups,[1] for which no effect of excitation wavelength was observed.[20] In methanol and ethylene glycol, however, the peridinin lifetimes after excitation into the higher vibrational levels of the S_2 state (425 nm) and into the very red edge of the S_0-S_2 transition (550 nm) are markedly changed. Interestingly, in acetonitrile, there is no effect of excitation wavelength on the peridinin lifetime, although this solvent is even more polar than methanol (Table 1), and both the rise (~0.6 ps) and decay (~8 ps) of the 950-nm signal are the same over the whole range of excitation wavelengths. This shows that solvent polarity is not a key parameter for the observed excitation wavelength dependence. Besides the results presented in Figure 3, the same excitation wavelength dependence is observed when probing either the S_1-S_2 transition at 1700 nm or the S_1/ICT-S_n transition at 600 nm (data not shown). Therefore, in methanol and ethylene glycol, shortening of the lifetimes following excitation into the red edge of the peridinin absorption spectrum is not limited to the ICT emission but it is exhibited at all wavelengths.

Deeper insight into the excitation wavelength dependence can be acquired by measuring transient absorption spectra of peridinin after excitation at different wavelengths. In Figure 4

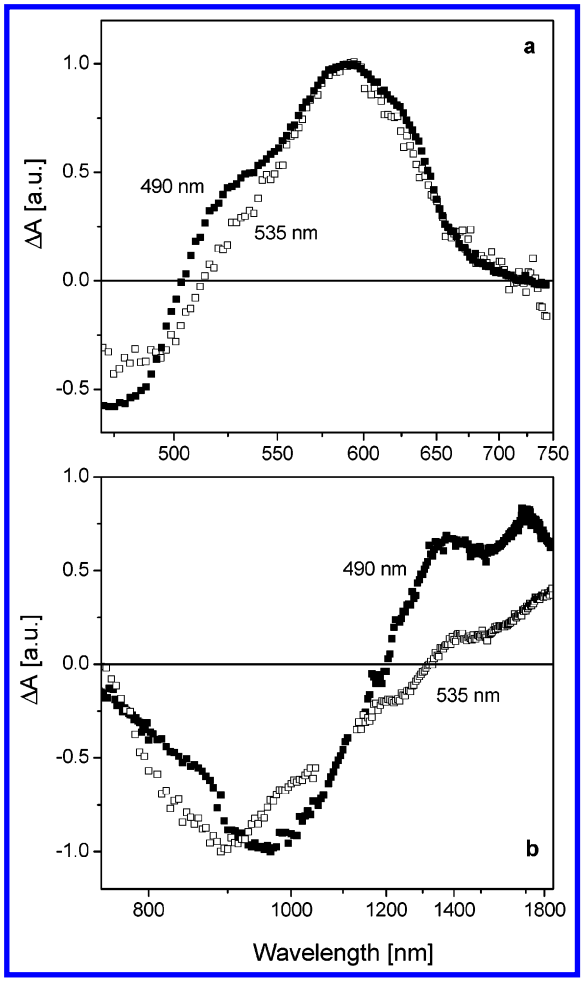

Figure 4. Transient absorption spectra of peridinin in methanol recorded in the visible (a) and the near-infrared (b) spectral regions after excitation at 490 nm (■) and at 535 nm (□). The transient absorption spectra in the visible region are normalized to the ESA maximum, whereas the near-infrared spectra are normalized to a maximum of the ICT emission.

are shown transient absorption spectra of peridinin in methanol excited at 490 and 535 nm recorded 1 ps after excitation. At this time delay, most of the peridinin molecules are in their S_1/ICT state because the S_2-S_1 relaxation occurs on a time scale shorter than 100 fs, as shown in Figure 5, where the kinetics of the S_2-S_1 relaxation are recorded for peridinin in methanol with a time resolution of ~30 fs.[21] Fitting the rise of the S_1/ICT-S_n signal at 630 nm yields a time constant of 56 fs, confirming that at 1 ps all of the relaxation processes involving higher excited states are finished. The transient absorption spectra in the visible region (Figure 4a) do not exhibit any striking

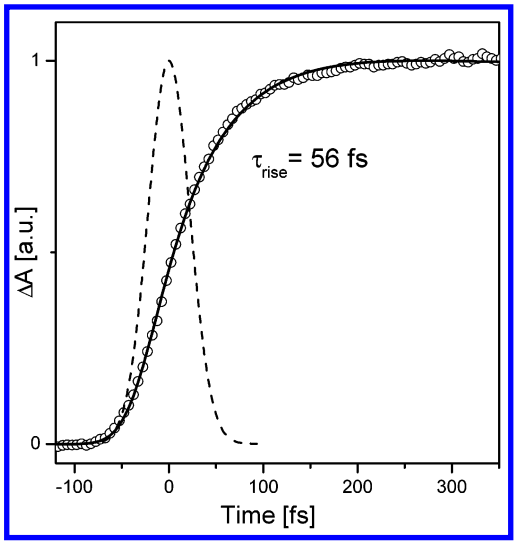

Figure 5. Rise of the S_1/ICT state of peridinin in methanol measured at 630 nm after 485-nm excitation with a better time resolution.[21] The solid line corresponds to a fit of the experimental data (○). The dashed line represents a Gaussian fit of the 50-fs response function.

differences when peridinin is excited at different wavelengths. The spectra are dominated by a strong ESA assigned previously to a mixture of the S_1/ICT-S_n transitions.[1,11] The shoulder at 525 nm, previously ascribed to the S_1-S_n transition,[11] is less pronounced following excitation at 535 nm, suggesting a decrease in the S_1 contribution. This loss of the S_1 signal is confirmed by the near-infrared transient absorption spectrum, where more pronounced changes are detected. For both excitations, the dominating feature is a negative band located at around 950 nm that was ascribed to a stimulated emission from the ICT state of peridinin.[12] The ICT emission band is slightly broader and blue-shifted when excited at 535 nm, but it is clear that the shift of the excitation toward red does not produce any significant changes of the ICT emission band shape. Nevertheless, the ESA signals corresponding to the 0−2 (1350 nm) and the 0−1 (1700 nm) vibrational bands of the S_1-S_2 transition[12] decreased by a factor of approximately 2 as compared with their magnitudes after 490-nm excitation. This is also consistent with a reduced S_1 contribution after excitation at 535 nm.

Transient absorption spectra of peridinin in methanol, ethylene glycol, and *n*-hexane in both visible and near-infrared regions are compared in Figure 6. For both polar solvents, peridinin was excited slightly below the maximum of the absorption spectrum—at 490 nm in methanol and at 500 nm in ethylene glycol (i.e., at wavelengths where the effect of the excitation wavelength is small (Figure 3)). The overall shape of the transient absorption spectra in the visible region is similar in both polar solvents, although in ethylene glycol it is shifted to the red by about 600 cm^{-1}, reflecting the red shift of the steady-state absorption spectrum shown in Figure 1. There is also a slightly less pronounced 525-nm shoulder in ethylene glycol. The fact that the methanol-to-ethylene glycol solvent change produces effects similar to those of the shift in the excitation wavelength in methanol is further verified by the near-infrared transient absorption spectrum (Figure 6b). The ratio between the magnitudes of the SE band and the ESA in the wavelength range of 1300−1800 nm is markedly different. It is also worth noting that although the S_0-S_2 transition is red-shifted by ∼450 cm^{-1} in ethylene glycol as compared with that in methanol (Figure 1) there is no shift of the S_1-S_2 transition, as judged from the positions of the 0−2 and 0−1 vibrational bands. Within experimental error, these bands are located at 1350 and 1690

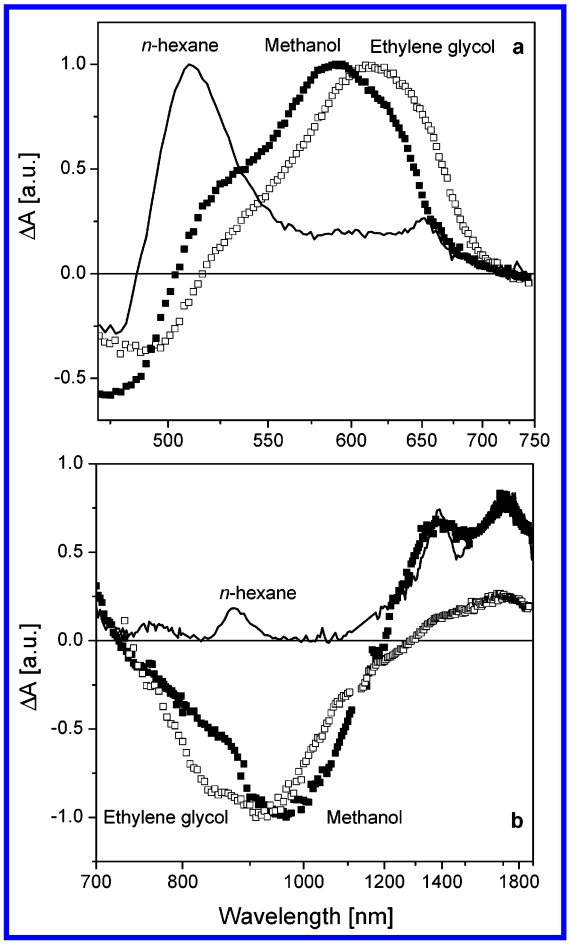

Figure 6. Transient absorption spectra of peridinin in *n*-hexane (—), methanol (■), and ethylene glycol (□) recorded in the visible (a) and the near-infrared spectral regions (b). For *n*-hexane and methanol, the excitation wavelength was at 490 nm, whereas 500 nm was used for ethylene glycol to account for a shift of the absorption spectrum. The transient absorption spectra in the visible region are normalized to the ESA maximum. In the near-infrared region, the spectra recorded in methanol and ethylene glycol are normalized to the ICT emission maximum, whereas the spectrum recorded in *n*-hexane is normalized to the maximum of the S_1-S_2 ESA in methanol.

nm, respectively, not only in polar solvents methanol and ethylene glycol but also in the nonpolar solvent *n*-hexane.

The effects of solvent viscosity on the excited states of peridinin were measured at three crucial wavelengths corresponding to the maximum of the S_1/ICT-S_n transition in the visible spectral region (600 nm), the maximum of the ICT stimulated emission (950 nm), and the S_1-S_2 transition in the infrared region (1700 nm). Results are presented in Figure 7. Despite the markedly different viscosities of methanol and ethylene glycol (see Table 1), the dynamics of the excited states of peridinin in both solvents are very similar. In methanol, the signals at all three wavelengths decay with a 9.6-ps time constant, whereas in ethylene glycol a slightly slower decay of 11.6 ps is observed. At 950 nm, which is the wavelength corresponding to the ICT emission, rise components of 1 ps (methanol) and 0.65 ps (ethylene glycol) are observed. This rise component is more pronounced in the case of peridinin in methanol. No 1-ps component is present in the kinetics recorded at 1700 nm, where in both methanol and ethylene glycol the observed signal rises within the response function. Kinetics measured at 600 nm possess both components because the ESA in the visible region consists of contributions from both the S_1 and ICT states.[1,11]

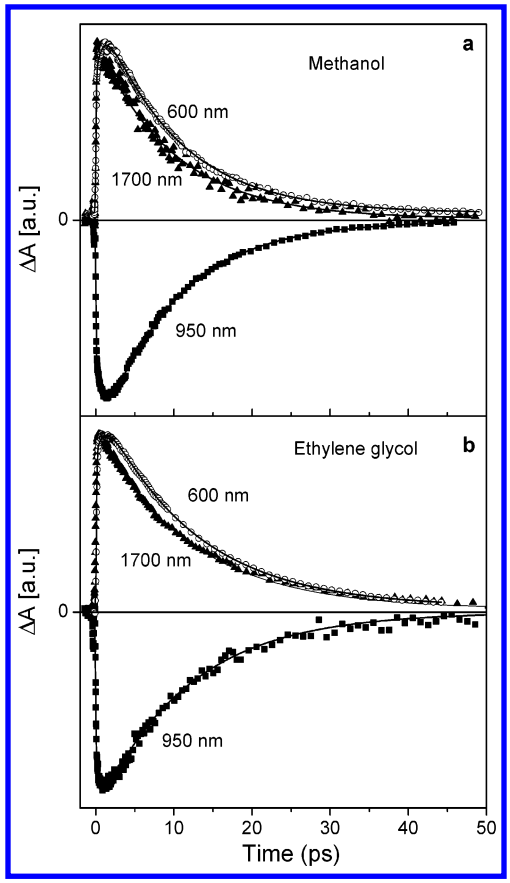

Figure 7. Kinetics recorded at 600 nm (○), 950 nm (■), and 1700 nm (▲) for peridinin in methanol (a) and ethylene glycol (b). The excitation wavelength was 490 nm for methanol and 500 nm for ethylene glycol. Solid lines represent fits.

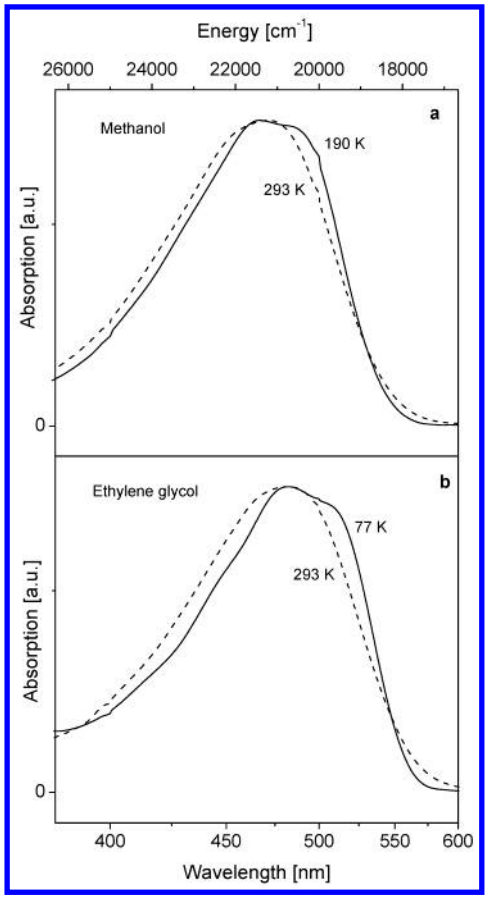

Figure 8. Absorption spectra of peridinin in (a) methanol at 293 K (– – –) and 190 K (—) and in (b) ethylene glycol at 293 K (– – –) and 77 K (—). All spectra are normalized to the maximum.

The temperature effect on the dynamics of the excited states of peridinin was studied in methanol and ethylene glycol. In methanol, experiments were performed at 190 K, ensuring that the sample was still in the liquid phase, whereas the ethylene glycol sample was frozen at 77 K, enabling us to study peridinin excited-state dynamics in a solid matrix. At low temperature, the vibrational structure of the S_0-S_2 transition in the steady-state absorption spectra is partially restored, and the spectra are narrower and red-shifted in both solvents (Figure 8).

The ICT state emission is present in both methanol and ethylene glycol even at low temperatures, and kinetics measured at the maximum (950 nm) of this band are shown in Figure 9. In methanol at 190 K, when the sample is still in the liquid phase, a significant prolongation of the peridinin lifetime is observed, and the decay remains monoexponential. The effect of excitation at different wavelengths is also pronounced at 190 K and is similar to that at 293 K. After excitation at 540 nm, the 950-nm signal decays with a 13-ps time constant, whereas after 500-nm excitation it is characterized by a 32-ps decay. The rise in the ICT state emission exhibits a similar trend to that observed at 293 K; the rise component is less pronounced after the red excitation. More complicated peridinin excited-state dynamics is detected at 77 K in an ethylene glycol glass, although the effect of the excitation wavelength is still pronounced. However, both with blue (480 nm) and red (540 nm) excitation, at least three decay components are necessary to obtain reasonable fits of the decays. The kinetics excited at both wavelengths were fitted globally, and the global fitting procedure gives the best results with time constants of 11, 53, and 205 ps. For the 480-nm excitation, all three decay components have similar amplitudes, but when excitation is into the red tail of the absorption spectrum at 540 nm, the longest component is negligible and the shortest component becomes the dominating one (see Table 3). Moreover, contrary to results at 293 K in ethylene glycol (see Figure 7), there is no observable rise in the ICT emission when peridinin is frozen in the ethylene glycol matrix.

4. Discussion

Two Forms of Peridinin in Protic Solvents. The results demonstrate that solvent polarity is not the only factor that affects the excited-state dynamics of peridinin. In addition to the previously observed shortening of the lifetime of the lowest excited state of peridinin due to an increase in the solvent polarity,[1,11,12] it is clear that other factors also modify the properties of the peridinin molecule. The most surprising result is the dependence of peridinin dynamics on excitation wavelength, which as shown in Figures 2 and 3 does not follow the solvent polarity. The peridinin lifetime markedly changes with excitation wavelength in methanol and ethylene glycol but not in acetonitrile, although all of these solvents have similar polarity (Table 1).

The data in Figures 2 and 3 suggest that more than one ground-state conformation of peridinin must exist in both methanol and ethylene glycol because the peridinin molecules excited below 500 nm exhibit different dynamics than those excited above 530 nm. The dependence of the lifetime on the excitation wavelength shown in Figure 3 can be well approximated by a sigmoidal shape, suggesting that it represents a transition between two different species. Indeed, the 950-nm kinetics following excitation at different wavelengths can also

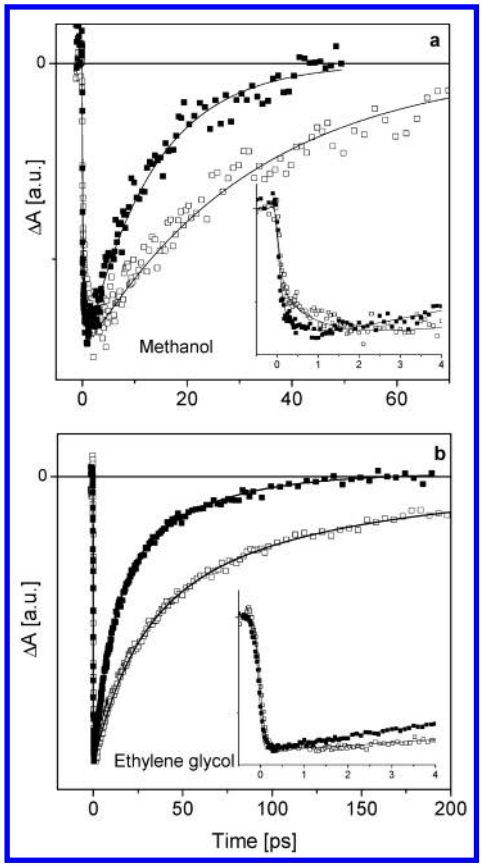

Figure 9. Kinetics recorded at 950 nm for peridinin in methanol (a) and in ethylene glycol (b) at low temperatures. For methanol at 190 K, kinetics were excited at 510 nm (open symbols) and 540 nm (solid symbols). For ethylene glycol, kinetics at 77 K were excited at 480 nm (open symbols) and 550 nm (solid symbols). In both panels, insets show the enlargement of the kinetics at early times after excitation. Solid lines going through the symbols represent fits of the low-temperature kinetics. All kinetics are normalized to their negative maximum.

TABLE 3: Time Constants and Amplitudes of Kinetic Components for Peridinin in Methanol at 190 K and in Ethylene Glycol Glass at 77 K[a]

λ_{exc} [nm]	τ_{rise} [ps]	A [%]	τ_1 [ps]	A_1 [%]	τ_2 [ps]	A_2 [%]	τ_3 [ps]	A_3 [%]
Methanol (190 K)								
510	0.9	*−40*	32	*100*				
540	0.6	*−25*	13	*100*				
Ethylene Glycol (77 K)								
480			11	*23*	53	*58*	206	*19*
550			11	*62*	53	*36*	206	*2*

[a] All kinetics were recorded at 950 nm. Negative amplitudes correspond to the rise components. Uncertainties of the amplitudes are within ±10%.

be successfully fitted globally (Table 4) with two decay components of 4.5 and 10.5 ps in methanol and 5.3 and 14.2 ps in ethylene glycol. In both solvents, the longer decay component dominates following excitation below 525 nm, whereas the shorter component is more significant following excitation at longer wavelengths. We suggest that two distinct peridinin species coexist in these solvents, which in the following discussion will be denoted as normal and red forms of peridinin. Because the red form of peridinin is most pronounced in ethylene glycol, another solvent parameter besides polarity that enhances the effect of the ICT state must exist. Comparing the parameters of the solvents, it seems that the hydrogen-bonding capability is directly related to the formation of the red peridinin form as demonstrated by the lack of excitation wavelength dependence in acetonitrile. In the protic solvents methanol and ethylene glycol, red peridinin is formed, most likely because of hydrogen bonding via the carbonyl group, and this effect is more pronounced in ethylene glycol with its two hydroxyl groups. Similar behavior was recently observed in a series of organic compounds, each of which possesses a carbonyl group in its structure, leading to ICT excited-state character.[22] It was shown that if a negative charge is localized on the carbonyl oxygen then significant ICT fluorescence quenching is achieved by intermolecular hydrogen bonding with ethanol. In peridinin, negative charge is expected to be mainly localized at the carbonyl oxygen,[1] in good agreement with the shorter peridinin lifetime in protic solvents. Thus, to achieve the strongest ICT character of the lowest excited state of peridinin, a solvent that is both polar and protic is needed.

A stronger effect of the ICT state in the case of the red peridinin form is also reflected in transient absorption spectra recorded after excitation into the blue and red parts of the absorption spectrum of peridinin in methanol (Figure 4). In the visible spectral region, the absence of the 525-nm shoulder in the transient absorption spectrum following excitation at 535 nm confirms that this band is indeed due to the S_1-S_n transition, as previously suggested.[1,11] Similarly, a significant decrease of the transient signal in the 1300−1800 nm region in the red-excited transient absorption spectrum assigns this ESA to the S_1-S_2 transition with only a minor contribution from the ICT state. However, the ESA band peaking at 590 nm and the broad stimulated emission band in the near-infrared region are clearly due to the ICT state.

The separation of signals originating from the S_1 and ICT states allows us to explore further the effect of different solvents. As shown in Figure 6, in *n*-hexane the S_1 contribution clearly dominates the transient absorption spectrum. Interestingly, although the highly viscous solvent ethylene glycol has about the same polarity as methanol (see Table 1), the transient absorption spectra taken in ethylene glycol exhibit a stronger ICT signal than that in methanol. This is clear from the ratio between the magnitudes of the ICT emission at 950 nm and the S_1-S_2 ESA at 1300−1800 nm, which represents the measure of the ICT state contribution to the transient signal. In fact, the normal form of peridinin in ethylene glycol exhibits about the same ICT signal as the red form in methanol. The normal form of peridinin in methanol clearly retains some of the features observed for peridinin in *n*-hexane, showing that the lowest excited state contains contributions from both the S_1 and ICT states. It is also demonstrated by the S_1 band located at 880 nm for peridinin in *n*-hexane (Figure 6), which is clearly superimposed on the ICT emission band following 490-nm excitation in methanol but is missing when excitation is shifted to 535 nm.

Spectral Broadening in Polar Solvents. The origin of the spectral broadening of the peridinin absorption in polar solvents can be explained by a change in the ground-state structure of the peridinin molecule. Recently, it was demonstrated by AM1 calculations that peridinin possesses a rather large ground-state dipole moment of 5.7 D.[1] As shown for substituted polyenes,[23] such dipolar ground-state character is enhanced by the solvent polarity, resulting in charge-transfer character. In polar aprotic solvents such as acetonitrile, spectral broadening is caused by an interaction of the peridinin molecule with the electric field of the solvent, leading to an absorption spectrum that is markedly broader than that in nonpolar solvent (Figure 1). In protic solvents, however, the dipolar character of the peridinin ground

TABLE 4: Global Fitting Amplitudes of Decay Components Measured at Room Temperature[a]

	methanol				ethylene glycol			
	$\lambda_{probe} = 950$ nm		$\lambda_{probe} = 1700$ nm		$\lambda_{probe} = 950$ nm		$\lambda_{probe} = 1700$ nm	
λ_{exc} [nm]	4.5-ps ampl [%]	10.5-ps ampl [%]	4.5-ps ampl [%]	10.5-ps ampl [%]	5.3-ps ampl [%]	14.2-ps ampl [%]	5.3-ps ampl [%]	14.2-ps ampl [%]
500	23	77	16	84	33	67	26	74
525	53	47	52	48	48	52	46	54
535	63	37	62	38	69	31	60	40
550	74	26	67	33	89	11	75	25

[a] Uncertainties of the amplitudes are within ±10%.

state is further enhanced by hydrogen bonding, producing an even more red-shifted absorption spectrum. Nevertheless, as pointed out by Frank et al.,[1] because peridinin has no specific electron-donor group (the conjugated chain itself is most likely acting as a weak electron donor), the changes in the ground-state dipole moment will be weaker than those observed for substituted polyenes having strong donor/acceptor groups. Consequently, these changes themselves cannot fully account for such a large broadening of the absorption spectrum of peridinin in polar solvents. In addition to the dipole-induced broadening, peridinin also exhibits conformational disorder in polar solvents,[1] which further broadens the peridinin absorption spectrum. This conformational broadening probably plays a major role in aprotic solvents, whereas in protic solvents the red tail of the absorption spectrum is due to the red form of peridinin having a larger ground-state dipole moment resulting from hydrogen bonding. It is clear that only a fraction of the peridinin molecules in a protic solvent can achieve the hydrogen-bound red form with stronger ICT character because the absorption spectrum in both methanol and ethylene glycol is still dominated by the normal peridinin form. Equilibrium is established between normal and red peridinin forms, and it is shifted more toward the red form in ethylene glycol because of its stronger hydrogen-bonding capacity.

In addition to the ground-state changes described above, it is possible that some of the observed changes in the absorption spectra in polar solvents could be caused by modifications of the S_2 state. A broadening of the absorption spectrum could be due to a mixing of the S_2 state with the S_1 and/or ICT states[24] because the S_1-S_2 energy gap is small for peridinin.[12] Mixing with other states in the vicinity of the S_2, such as the $1B_u^-$ or $3A_g^-$ state, revealed recently for other carotenoids by resonance Raman spectroscopy is also a possibility.[25,26] Nevertheless, a strong dependence of the energies of these states on conjugation length suggests that they should be markedly higher than the S_2 state for a carotenoid such as peridinin with eight carbon−carbon conjugated double bonds.[27] A better candidate for mixing could be the S* state found in spirilloxanthin[28] and spheroidene,[29] whose energy has a weaker dependence on the conjugation length than for the $1B_u^-$ and $3A_g^-$ states. However, the involvement of the S* state in peridinin dynamics is unlikely because the S* state was a precursor of picosecond triplet formation[28,29] and no triplet signal was found here. The two-photon excitation spectra of peridinin in benzene and in PCP indicate that the S_1/ICT-S_2 mixing is not changed by solvent polarity,[24] suggesting that the S_2 state is only marginally affected by polarity. This is further confirmed by the spectral profile of the S_1-S_2 ESA, which is very similar in both methanol and *n*-hexane (Figure 6), demonstrating that the change in the peridinin S_2 state due to polarity is too small to account for the distinct changes in the peridinin absorption spectrum between polar and nonpolar solvents.

Origin of the 1-ps Rise Component. In our previous paper,[12] two models treating S_1 and ICT as two separate states were considered. In the first model, the ~1-ps rise component represented the S_1-ICT transfer followed by an ~10-ps decay of the ICT state to the peridinin ground state. The second model involved a "reverse" ordering of the time constants, where the ~10-ps component was due to transfer over a polarity-controlled barrier between the S_1 and ICT states, whereas the ~1-ps component represented a fast ICT-S_0 relaxation due to strong coupling of the ICT and ground states. On the basis of a kinetic modeling of the recorded traces, we favored the second model because of its ability to explain the observed peridinin dynamics. However, the data presented above suggest that this model can hardly explain the new dynamical features reported here. According to our model, the shorter rise component observed for the red form of peridinin would require an unrealistically high ICT-S_0 transition dipole moment to account for a strong ICT emission. In addition, the rise component is completely lacking when peridinin is frozen in ethylene glycol glass (Figure 9). Therefore, we conclude that this rise component is not due to the ICT state relaxation, and the model described in ref 12 can be ruled out. Instead, a significant mixing of the S_1 and ICT states, as proposed by Frank et al.,[1] is most likely the appropriate model to explain the wavelength-independent peridinin lifetime. Such mixing will lead to a collective S_1/ICT state having both S_1 and ICT character, with the degree of ICT character depending on the solvent properties.

What then is the origin of the rise component observed in the 950-nm traces? This component is most pronounced for the normal form of peridinin, and its time constant clearly follows the solvent polarity.[12] It is not due to a reorientation of solvent molecules as a response to the change in the dipole moment of peridinin molecules after excitation because the rise times observed in different solvents do not match the known solvation times.[30] Interestingly, although the decrease in temperature to 190 K in methanol does not affect the rise component, freezing of the sample in ethylene glycol glass at 77 K causes its disappearance (Figure 9 and Table 3). Its presence only when peridinin is in the liquid phase indicates a connection with a conformational change in the excited state. Such a conformational change resulting in the increased ICT character of the S_1/ICT state could be described as a TICT mechanism. However, TICT state formation would be slowed by an increase in viscosity,[16] which is the opposite situation to that observed here. The rise component is 0.6 ps in ethylene glycol, whereas in methanol, having a viscosity of more than an order of magnitude lower, a 1-ps rise is observed. Overall, the peridinin dynamics exhibit only a small dependence on viscosity, comparable to that observed for the xanthophylls zeaxanthin and lutein.[31] These do not contain a carbonyl group and therefore do not exhibit any polarity-dependent behavior.[1] This confirms that no twisting of terminal groups is involved in the excited-state dynamics of peridinin; consequently, the rise component of the ICT state emission cannot be assigned to the TICT mechanism. Although no molecular twisting is involved, the rise component is most likely connected with a small structural change of the peridinin

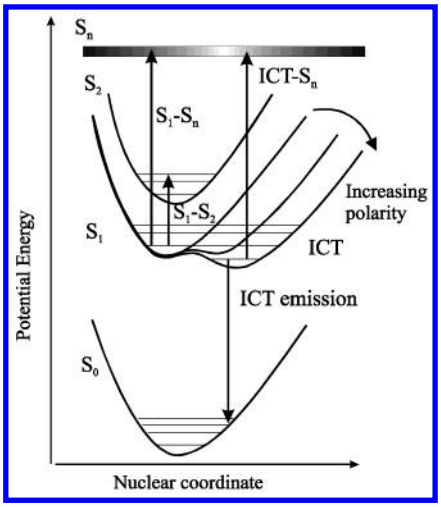

Figure 10. Potential energy surface diagram showing the polarity effect on the structure of the S_1/ICT potential surface of the peridinin molecule. The transitions corresponding to the observed signals are denoted by arrows. Because of the lack of knowledge about the S_n potential surface, it is visualized only as a line representing a final state for S_1-S_n and ICT-S_n transitions. See the text for details.

molecule in the excited state. It was previously shown that if the groups that are involved in structural changes leading to an enhancement of the ICT state emission are small then viscosity has no effect.[16] Because this process is exhibited as a rise in the ICT state emission, it is likely that the carbonyl group changes its orientation slightly to stabilize the strongest possible ICT character of the lowest excited state. It is most pronounced for the normal form of peridinin, where the carbonyl group is free to move to enhance the ICT character of the S_1/ICT state. For the red form of peridinin in protic solvents, the carbonyl group is involved in hydrogen bonding with the solvent; consequently, its ability to change its orientation is limited. This results in a suppression of the rise component in the red peridinin form. In the case of peridinin in the solid phase at 77 K in ethylene glycol, the movement of the molecule is prevented, and no rise component is observed. It is important to note that although this conformational change leads to stronger ICT character it is not a transfer between the S_1 and ICT states as proposed in one of the earlier models.[12] It is more a change of the S_1/ICT potential surface leading to increased ICT character.

Model of Peridinin Excited States. On the basis of the described dynamical features, we have constructed a model, which is depicted in Figure 10. Except for a few modifications, it is in good agreement with that proposed by Frank et al.[1] Peridinin's lowest excited state has a complicated potential surface whose shape is determined by the degree of mixing between the S_1 and ICT states, which is related to solvent polarity. We propose that in nonpolar solvents the lowest excited state has purely S_1 character. With an increase in solvent polarity, the S_1/ICT state gains more ICT character, making the potential surface broader. This broadening leads to the appearance of the characteristic ICT emission, which is significantly red-shifted from the S_1 emission because of a considerable shift between the ICT and S_0 potential minima. In addition, the ICT part of the potential surface is the origin of the strong and broad ESA band appearing around 600 nm for peridinin in polar solvents (Figure 6). However, opening the ICT part of the potential surface decreases the S_1-S_2 signal because a fraction of the S_1/ICT population is moved toward the ICT part, as is clearly noticeable in Figure 6b.

The S_1-like and ICT-like minima of the S_1/ICT potential surface are separated by a low, polarity-controlled barrier. When polarity reaches a certain value, the barrier is low enough to allow thermal coupling and a high degree of ICT character of the S_1/ICT state. A separation of the S_1-like and ICT-like minima by a low barrier is also the reason for the observed uniform peridinin lifetime over a broad range of wavelengths. It is further supported by the temperature dependence (Figure 9 and Table 3) because a decrease in temperature has a similar effect on the S_1/ICT lifetime as a decrease in solvent polarity. It is significant that the temperature dependence of the S_1 lifetime of peridinin is much more pronounced than that of the S_1 lifetime of the non-carbonyl carotenoid spheroidene, which is only about 20% longer at 190 K than at 293 K.[18] In peridinin at sufficiently low temperature, the barrier is too high for coupling between the S_1 and ICT states, and the S_1/ICT lifetime is close to that observed in a nonpolar solvent, as shown for peridinin at 77 K in ethylene glycol glass: a small fraction of molecules is frozen in a conformation with little ICT character, leading to an S_1/ICT lifetime of 200 ps (Table 3). This 200-ps component is negligible after 550-nm excitation, in good agreement with the hypothesis that the red tail of the absorption spectrum is caused by the absorption of peridinin molecules with strong ICT character. In addition, similar behavior has been observed for dicyano-apo-β-carotene, for which identical lifetimes in polar and nonpolar solvent were observed at 4.2 K, although they were significantly different at 293 K.[14]

Because signals characteristic of both S_1 and ICT states are observed for normal peridinin in methanol, the energy difference between the potential minima corresponding to the S_1 and ICT parts of the S_1/ICT potential surface must be very small. If the ICT minimum were significantly lower, then most of the S_1/ICT population would be transferred toward this minimum of the potential surface, resulting in a loss of the S_1 contribution. In protic solvents, hydrogen bonding via the carbonyl group further stabilizes the ICT character of the S_1/ICT state, pushing the ICT minimum slightly lower than that of the S_1, resulting in a shift of the equilibrium toward the ICT state.

It is necessary to emphasize that Figure 10 represents a model for only one particular peridinin conformation. As discussed above, a distribution of peridinin conformers exists in polar solvents. Each of these different conformations has slightly different excited-state properties, as demonstrated by different conformers frozen in ethylene glycol glass. Apparently, for some conformers the S_1-ICT barrier is higher than that for others, leading to a multiexponential decay of the S_1/ICT state. A slight structural change in the excited state is also responsible for the rise component observed in polar solvents; thus these features cannot be included in the model depicted in Figure 10 because they include a change in the S_1/ICT potential surface. In protic solvents, the dynamics of peridinin is further complicated because hydrogen bonding leads to the formation of a red peridinin form with different properties of both ground and excited states. However, a reduction of the 950-nm rise component suggests that hydrogen bonding is a limiting factor for the change of conformation in the excited state, although it is likely that even the red form of peridinin still exhibits some distribution of ground-state conformers.

A key question is how the complicated dynamics of peridinin in solution relates to its behavior in the PCP complex because the S_1/ICT state is directly involved in energy transfer between peridinin and Chl-*a*.[32] Interestingly, both the steady-state and transient absorption spectra of peridinin in the PCP complex well resemble those recorded in the polar and protic solvent ethylene glycol, indicating the strong ICT character of the S_1/ICT state in the protein.[32] The PCP complex contains polar

hydrogen-bonding residues as well as a number of water molecules.[3] Such a combination of the proper conformation and hydrogen bonding leads to the strong ICT character of the S_1/ICT state, providing an efficient energy transfer via the S_1/ICT state.

Acknowledgment. We thank Yuri Zaushitsyn for technical assistance with the measurements with 30-fs time resolution, Frank Sharples for his expertise in HPLC, and Harry Frank for useful discussions. The work at Lund University was performed with funding from the Swedish Research Council, the Wallenberg Foundation, and the Crafoord Foundation. R.G.H. was supported by the Australian Research Council (project grant A00000264), and T.P., by DESS (Delegationen för Energiförsörjning i Sydsverige).

References and Notes

(1) Frank, H. A.; Bautista, J. A.; Josue, J.; Pendon, Z.; Hiller, R. G.; Sharples, F. P.; Gosztola, D.; Wasielewski, M. R. *J. Phys. Chem. B* **2000**, *104*, 4569.

(2) Hiller, R. G. In *Photochemistry of Carotenoids*; Frank, H. A., Young, A. J., Britton, G., Cogdell, R. J., Eds.; Kluwer Academic Publishers: Dordrecht, The Netherlands, 1999; p 81.

(3) Hofmann, E.; Wrench, P.; Sharples, F. P.; Hiller, R. G.; Welte, W.; Diederichs, K. *Science* **1996**, *272*, 1788.

(4) Bautista, J. A.; Hiller, R. G.; Sharples, F. P.; Gosztola, D.; Wasielewski, M.; Frank, H. A. *J. Phys. Chem. A* **1999**, *103*, 2267.

(5) Krueger, B. P.; Lampoura, S. S.; van Stokkum, I. H. M.; Papagiannakis, E.; Salverda, J. M.; Gradinaru, C. C.; Rutkauskas, D.; Hiller, R. G.; van Grondelle, R. *Biophys. J.* **2001**, *80*, 2843.

(6) Damjanović, A.; Ritz, T.; Schulten, K. *Biophys. J.* **2000**, *79*, 1695.

(7) Ritz, T.; Damjanović, A.; Schulten, K.; Zhang, J.-P.; Koyama, Y. *Photosynth. Res.* **2000**, *66*, 125.

(8) van Amerongen, H.; van Grondelle, R. *J. Phys. Chem. B* **2001**, *105*, 604.

(9) Christensen, R. L. In *Photochemistry of Carotenoids*; Frank, H. A., Young, A. J., Britton, G., Cogdell, R. J., Eds.; Kluwer Academic Publishers: Dordrecht, The Netherlands, 1999; p 137.

(10) Mimuro, M.; Nagashima, U.; Takaichi, S.; Nishimura, Y.; Yamazaki, I.; Katoh, T. *Biochim. Biophys. Acta* **1992**, *1098*, 271.

(11) Bautista, J. A.; Connors, R. E.; Raju, B. B.; Hiller, R. G.; Sharples, F. P.; Gosztola, D.; Wasielewski, M. R.; Frank, H. A. *J. Phys. Chem. B* **1999**, *103*, 8751.

(12) Zigmantas, D.; Polívka, T.; Yartsev, A.; Hiller, R. G.; Sundström, V. *J. Phys. Chem. A.* **2001**, *105*, 10296.

(13) He, Z.; Gosztola, D.; Deng, Y.; Gao, G.; Wasielewski, M.; Kispert, L. D. *J. Phys. Chem B* **2000**, *104*, 6668.

(14) O'Neil, M. P.; Wasielewski, M. R.; Khaled, M. M.; Kispert, L. D. *J. Chem. Phys.* **1991**, *95*, 7212.

(15) Polívka, T.; Herek, J. L.; Zigmantas, D.; Åkerlund, H.-E.; Sundström, V. *Proc. Natl. Acad. Sci. U.S.A.* **1999**, *96*, 4914.

(16) Bhattachryya, K.; Chowdhury, M. *Chem. Rev.* **1993**, *93*, 507.

(17) Plaza, P.; Laage, D.; Martin, M. M.; Alain, V.; Blanchard-Desce, M.; Thompson, W. H.; Hynes, J. T. *J. Phys. Chem. A* **2000**, *104*, 2396.

(18) Polívka, T.; Zigmantas, D.; Frank, H. A.; Bautista, J. A.; Herek, J. L.; Koyama, Y.; Fujii, R.; Sundström, V. *J. Phys. Chem. B* **2001**, *105*, 1072.

(19) Zhang, J.-P.; Skibsted, L. H.; Fujii, R.; Koyama, Y. *Photochem. Photobiol.* **2001**, *73*, 219.

(20) Frank, H. A.; Desamero, R. Z. B.; Chynwat, V.; Gebhard, R.; van der Hoef, I.; Jansen, F. J.; Lugtenburg, J.; Gosztola, D.; Wasielewski, M. R. *J. Phys. Chem. A* **1997**, *101*, 149. Although we are not aware of any systematic study of wavelength dependence for non-carbonyl carotenoids, the S_1 lifetime of spheroidene excited at 490 nm (ref 18) and at 400 nm (this reference) shows that the lifetime does not depend on the excitation wavelength.

(21) Measurements with 30-fs time resolution were carried out with a different laser system consisting of a 1-kHz Ti:sapphire amplifier and two noncollinear optical parametric amplifiers. For details, see Kallioinen, J.; Benkö, G.; Sundström, V.; Korpi-Tommola, J.; Yartsev, A. P. *J. Phys. Chem. B* **2002**, *106*, 4396.

(22) Morimoito, A.; Yatsuhashi, T.; Shimada, T.; Biczók, L.; Tryk, D. A.; Inoue, H. *J. Phys. Chem. A* **2001**, *105*, 10488.

(23) Bublitz, G. U.; Ortiz, R.; Marder, S. R.; Boxer, S. G. *J. Am. Chem. Soc.* **1997**, *119*, 3365.

(24) Zimmermann, J.; Linden, P. A.; Vaswani, H. M.; Hiller, R. G.; Fleming, G. R. *J. Phys. Chem. B* **2002**, *106*, 9418.

(25) Sashima, T.; Koyama, Y.; Yamada, T.; Hashimoto, H. *J. Phys. Chem. B* **2000**, *104*, 5001.

(26) Furuichi, K.; Sashima, T.; Koyama, Y. *Chem. Phys. Lett.* **2002**, *356*, 547.

(27) Tavan, P.; Schulten, K. *Phys. Rev. B* **1987**, *36*, 4337.

(28) Gradinaru, C. C.; Kennis, J. T. M.; Papagiannakis, E.; van Stokkum, I. H. M.; Cogdell, R. J.; Fleming, G. R.; Niederman, R. A.; van Grondelle, R. *Proc. Natl. Acad. Sci. U.S.A.* **2001**, *98*, 2364.

(29) Papagiannakis, E.; Kennis, J. T. M.; van Stokkum, I. H. M.; Cogdell, R. J.; van Grondelle, R. *Proc. Natl. Acad. Sci. U.S.A.* **2002**, *99*, 6017.

(30) Horng, M. L.; Gardecki, J. A.; Papazyan, A.; Maroncelli, M. *J. Phys. Chem.* **1995**, *99*, 17311.

(31) Holt, N.; Ma, Y. Z.; Fleming, G. R. Results presented at the 13th International Carotenoid Symposium, Honolulu, Hawaii, 2002.

(32) Zigmantas, D.; Hiller, R. G.; Sundström, V.; Polívka, T. *Proc. Natl. Acad. Sci. U.S.A.* **2002**, *99*, 16760.